


 Cite this: *React. Chem. Eng.*, 2020, 5, 1237

Tungsten–zirconia-supported rhenium catalyst combined with a deoxydehydration catalyst for the one-pot synthesis of 1,4-butanediol from 1,4-anhydroerythritol†

 Tianmiao Wang,^a Yoshinao Nakagawa,^{id} *^{ab} Masazumi Tamura,^{id} ‡^{ab}
 Kazu Okumura^c and Keiichi Tomishige^{id} *^{ab}

Efficient and reusable catalysts were developed for one-pot reduction of 1,4-anhydroerythritol (1,4-AHery), which is a promising biomass-derived C4 platform chemical, into 1,4-butanediol (1,4-BuD) with H₂. First, various ReO_x catalysts on oxide supports were tested for reductive conversion of 2,5-dihydrofuran (2,5-DHF) to 1,4-butanediol (1,4-BuD). ReO_x/WO₃–ZrO₂ showed the best performance, and ReO_x catalysts supported on other oxides were much less active in the isomerization of 2,5-DHF to 2,3-DHF which is the first step of the 2,5-DHF conversion to 1,4-BuD. The ReO_x/WO₃–ZrO₂ catalyst was combined with the ReO_x–Au/CeO₂ catalyst for deoxydehydration (DODH) of 1,4-AHery into 2,5-DHF to develop a one-pot conversion system of 1,4-AHery to 1,4-BuD. The highest 1,4-BuD yield of 55% from 1,4-AHery was obtained. Even though the yield was lower than that obtained over the combination of ReO_x/C and ReO_x–Au/CeO₂ catalysts in our previous study, the regeneration of the combination of ReO_x/WO₃–ZrO₂ and ReO_x–Au/CeO₂ is possible: calcination at 573 for 3 h of the used catalyst mixture increased the activity to the fresh level. THF was the major by-product in both 1,4-AHery and 2,5-DHF conversions, which was due to hydrogenation of DHF, disproportionation of DHF and/or dehydration of 1,4-BuD. The W amount in WO₃–ZrO₂ greatly affected the catalytic performance of ReO_x/WO₃–ZrO₂: too much W above the monolayer level on the ZrO₂ support sharply decreased the activity in 2,5-DHF isomerization. On the other hand, WO₃–ZrO₂ with a tetragonal ZrO₂ structure prepared by co-precipitation showed comparable performance to WO₃–ZrO₂ with a monoclinic ZrO₂ structure as the support of the ReO_x catalyst, demonstrating that the crystal structure of ZrO₂ has little effect on the catalytic performance. The Re species were suggested to be highly dispersed on the WO₃ (sub)monolayer on ZrO₂ based on the effect of the Re loading amount. The dispersed Re species on monolayer WO₃ species on ZrO₂ can be the active sites for 2,5-DHF disproportionation to 2,3-DHF.

 Received 4th March 2020,
 Accepted 11th May 2020

DOI: 10.1039/d0re00085j

rsc.li/reaction-engineering

Introduction

Biomass plays an increasingly significant role as a chemical feedstock and energy resource instead of fossil fuels due to

the depletion of oil and natural gas. Although biomass-derived products are more sustainable and renewable, most of them are not convenient and economical as feedstocks for energy generation or the chemical industry due to the high oxygen content.^{1–5} Catalytic conversions such as selective C–O hydrogenolysis (dissociation of the C–O bond and addition of hydrogen atoms from H₂) of biomass-based chemicals can effectively reduce the oxygen numbers and increase their commodity value. Sugar alcohols, such as glycerol, erythritol, xylitol, and sorbitol, are biomass-derived compounds widely used as sweeteners instead of sugar in the food industry. They can be produced on the industrial scale and have large feedstock supply. As platform chemicals, sugar alcohols can be converted to value-added chemicals by selectively removing OH groups,⁶ for example, glycerol can be converted to 1,3-propanediol or

^a Department of Applied Chemistry, School of Engineering, Tohoku University, 6-6-07 Aoba, Aramaki, Aoba-ku, Sendai, 980-8579, Japan.

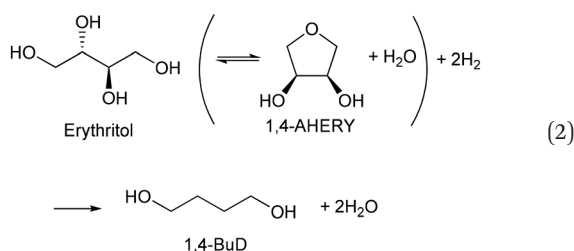
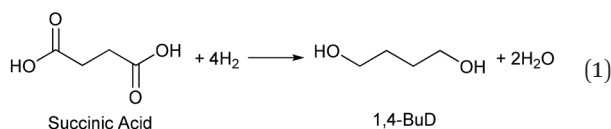
E-mail: yoshinao@erec.che.tohoku.ac.jp, tomi@erec.che.tohoku.ac.jp

^b Research Center for Rare Metal and Green Innovation, Tohoku University, 468-1 Aoba, Aramaki, Aoba-ku, Sendai, 980-0845, Japan

^c Department of Applied Chemistry, Faculty of Engineering, Kogakuin University, 2665-1 Nakano-machi, Hachioji, Tokyo 192-0015, Japan

† Electronic supplementary information (ESI) available. See DOI: 10.1039/d0re00085j

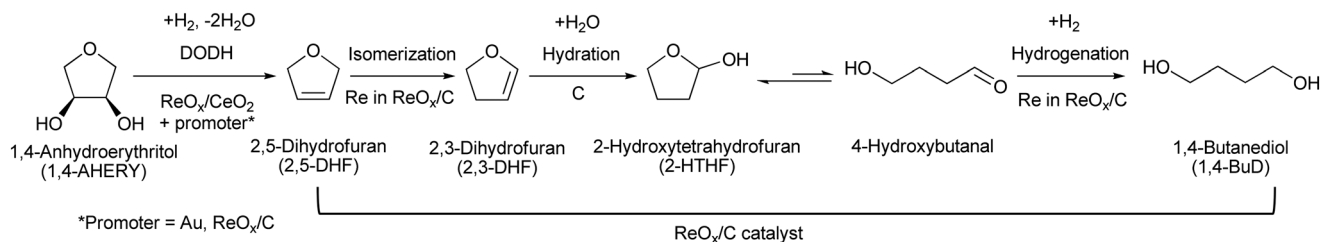
‡ Current address: Research Center for Artificial Photosynthesis, The Advanced Research Institute for Natural Science and Technology, Osaka City University, 3-3-138 Sugimoto, Sumiyoshi, Osaka, 558-8585, Japan.



Recently, we have reported that 1,4-BuD could be produced from 1,4-AHRY over the combination of ReO_x/C and $\text{ReO}_x\text{-Au/CeO}_2$ catalysts in a one-pot reaction.²³ The yield of 1,4-BuD was around 90% which was the highest

yield of 1,4-BuD from biomass-derived products so far even including succinic acid. In this co-catalyst system, $\text{ReO}_x\text{-Au/CeO}_2$ firstly catalyzed the reduction of 1,4-AHERY to 2,5-dihydrofuran (2,5-DHF), and $\text{ReO}_x\text{/C}$ catalyzed the further reduction of 2,5-DHF to 1,4-BuD (Scheme 1). The former step is the conversion of *cis*-vicinal OH groups to a C=C double bond which is called deoxydehydration (DODH), and this reaction is typically catalyzed by homogeneous $\text{Re}(\text{VII})$ catalysts with organic reducing agents such as 3-pentanol and PPh_3 .^{24–26} Development of solid catalysts for DODH has been a hot topic in biomass conversion.^{27–31} Our laboratory has developed a heterogeneous $\text{ReO}_x\text{-Au/CeO}_2$ catalyst for DODH using H_2 as the reducing agent.^{32–35} The highly dispersed monomeric Re oxide species on the crystalline CeO_2 surface can be the active sites of DODH.^{32,33,36–38} Au serves as the activation site of H_2 , and the activated hydrogen species move on CeO_2 probably as pairs of protons and electrons to Re species. Au was selected among various noble metals based on its low C=C hydrogenation activity.³² The stabilization of high valent Re species by CeO_2 and the capability of hydrogen species to move on the CeO_2 surface are the keys of the DODH activity. The latter step catalyzed by $\text{ReO}_x\text{/C}$ consists of the following steps: the isomerization of 2,5-DHF to 2,3-dihydrofuran (2,3-DHF), the hydration of 2,3-DHF to 2-hydroxytetrahydrofuran (2-HTHF), and the reduction of 2-HTHF or its straight chain form 4-hydroxybutanal to 1,4-BuD. In the most recent research, we also found that the $\text{ReO}_x\text{/CeO}_2$ catalyst without an Au promoter still could catalyze the DODH reaction in the presence of $\text{ReO}_x\text{/C}$, enabling the reduction of 1,4-AHERY to 1,4-butanediol with the mixture of $\text{ReO}_x\text{/CeO}_2$ and $\text{ReO}_x\text{/C}$.³⁹ The Re species on carbon could activate H_2 like an Au promoter for the reduction of Re species on the CeO_2 surface which are the active sites in the conversion of 1,4-AHERY. Furthermore, CeO_2 without Re loading combined with $\text{ReO}_x\text{/C}$ even could convert 1,4-AHERY to 1,4-BuD, because the Re species on the carbon surface could move to CeO_2 surfaces to form $\text{ReO}_x\text{/CeO}_2$. The highest yield of 1,4-BuD reached 85% over the $\text{ReO}_x\text{/CeO}_2 + \text{ReO}_x\text{/C}$ system, which was comparable to that in the co-catalyst system with an Au promoter. As above, $\text{ReO}_x\text{/C}$ plays many roles in this system: C=C bond movement (isomerization), H_2 activation, hydrolysis and C=O hydrogenation. Versatile roles of $\text{ReO}_x\text{/C}$ have been also reported in other catalytic reactions with multiple steps such as reductive lignin depolymerization.^{40,41}

The largest drawback of these mixed catalyst systems was catalyst deactivation. The conversion of 1,4-AHERY sharply dropped from 100% to 65% ($\text{ReO}_x\text{-Au/CeO}_2 + \text{ReO}_x/\text{C}$) or 64% ($\text{ReO}_x/\text{CeO}_2 + \text{ReO}_x/\text{C}$) after the first run in reuse tests, indicating the deactivation of $\text{ReO}_x\text{(-Au)/CeO}_2$. The selectivity to 1,4-BuD also decreased, indicating the deactivation of ReO_x/C . The activity of noble-metal-modified $\text{ReO}_x/\text{CeO}_2$ catalysts for DODH has been also reported to be deactivated during the reaction; however, they can be regenerated by calcination to recover the activity.³² On the



Scheme 1 One-pot conversion of 1,4-AHERY to 1,4-BuD over $\text{ReO}_x(-\text{Au})/\text{CeO}_2 + \text{ReO}_x/\text{C}$.

other hand, due to the combustibility of the carbon support, it is not feasible to regenerate the recycled catalyst mixture by calcination. Therefore, in this study, a new Re catalyst with a regenerable support was studied as an alternative to ReO_x/C in the co-catalyst system with $\text{ReO}_x-\text{Au}/\text{CeO}_2$. Among various oxide-supported ReO_x catalysts, $\text{ReO}_x/\text{WO}_3-\text{ZrO}_2$ is a possible alternative to ReO_x/C combined with $\text{ReO}_x-\text{Au}/\text{CeO}_2$ in the production of 1,4-BuD from 1,4-AHERY. While the yield of 1,4-BuD over the combination of $\text{ReO}_x/\text{WO}_3-\text{ZrO}_2 + \text{ReO}_x-\text{Au}/\text{CeO}_2$ was lower than that over the co-catalyst with a carbon support, the activity of the used catalyst mixture of $\text{ReO}_x/\text{WO}_3-\text{ZrO}_2$ and $\text{ReO}_x-\text{Au}/\text{CeO}_2$ could be regenerated by calcination, which could be comparable to the fresh one.

Experimental section

The $\text{ReO}_x/\text{support}$ catalysts were prepared by impregnating the support materials with NH_4ReO_4 (Mitsui Chemicals Co. Ltd.) aqueous solution at 353 K. The support materials included commercial ZrO_2 (Daiichi Kigenso Kagaku Kogyo Co., Ltd., BET surface area: $62 \text{ m}^2 \text{ g}^{-1}$), C (Cabot Co., carbon black BP2000, $1282 \text{ m}^2 \text{ g}^{-1}$), TiO_2 (Aerosil Co. Ltd., P25, $47 \text{ m}^2 \text{ g}^{-1}$), SiO_2 (Fuji Silysia Co. Ltd., G-6, BET surface area: $535 \text{ m}^2 \text{ g}^{-1}$), Al_2O_3 (Aerosil Co. Ltd., 87 $\text{m}^2 \text{ g}^{-1}$), MgO (Ube Industries, Ltd., 500A, $34 \text{ m}^2 \text{ g}^{-1}$), HZSM-5 (JRC-Z5-90H(1), Süd-Chemie Catalysts and Catalysis Society of Japan, $\text{Si}/\text{Al}_2 = 90$, $390 \text{ m}^2 \text{ g}^{-1}$), $\text{TiO}_2-\text{ZrO}_2$ ($\text{TiO}_2 = 30 \text{ wt\%}$, Daiichi Kigenso Kagaku Kogyo Co., Ltd., $148 \text{ m}^2 \text{ g}^{-1}$), $\text{SiO}_2-\text{ZrO}_2$ ($\text{SiO}_2 = 10 \text{ wt\%}$, Daiichi Kigenso Kagaku Kogyo Co., Ltd., $136 \text{ m}^2 \text{ g}^{-1}$), $\text{CeO}_2-\text{ZrO}_2$ ($\text{CeO}_2 = 50 \text{ wt\%}$, Daiichi Kigenso Kagaku Kogyo Co., Ltd., $136 \text{ m}^2 \text{ g}^{-1}$), and WO_3-ZrO_2 ($\text{WO}_3 = 10 \text{ wt\%}$, Daiichi Kigenso Kagaku Kogyo Co., Ltd., $103 \text{ m}^2 \text{ g}^{-1}$). All these supports were calcined at 773 K for 3 h before impregnation. The Re loading amount was 3 wt% and 1 wt% for single-component supports and mixed oxide supports, respectively, unless noted. Other tungsten-zirconia catalysts were also used. $^{\text{cP}}\text{WO}_3-\text{ZrO}_2$ ($\text{W} = 5 \text{ wt\%}$) was prepared by a co-precipitation method using zirconium nitrate oxide dihydrate (Kanto Chemical Co. Inc.),

ammonium metatungstate hydrate (Strem Chemicals Inc.) and ammonia water (0.1 M). The addition of ammonia water was carried out at 353 K, and the precipitate was filtered, dried in an oven at 373 K for 12 h, and finally calcined at 773 K for 3 h. The BET surface area of $^{\text{cP}}\text{WO}_3-\text{ZrO}_2$ was $68 \text{ m}^2 \text{ g}^{-1}$. The $\text{ReO}_x/^{\text{cP}}\text{WO}_3-\text{ZrO}_2$ catalyst (Re 1 wt%) was prepared by impregnation of $^{\text{cP}}\text{WO}_3-\text{ZrO}_2$ with NH_4ReO_4 . The $\text{ReO}_x/\text{WO}_3/\text{support}$ catalysts (Re 1 wt%) were prepared by the sequential impregnation method. The $\text{WO}_3/\text{support}$ was firstly prepared by impregnating the supports, including ZrO_2 , Al_2O_3 , and TiO_2 , with ammonium metatungstate hydrate aqueous solution at 353 K. The $\text{WO}_3/\text{support}$ samples were dried (373 K, 12 h), calcined (773 K, 3 h) and then impregnated with NH_4ReO_4 aqueous solution at 353 K. All the impregnated catalysts were dried in an oven at 373 K for 12 h, and then calcined 773 K for 3 h. The $\text{ReO}_x-\text{Au}/\text{CeO}_2$ (1 wt% Re, 0.3 wt% Au) catalyst was prepared by a deposition-precipitation method for Au loading and subsequent impregnation for Re loading according to the previous report.³²

The activity test was conducted with an autoclave reactor equipped with an inner glass cylinder. After the reaction, both gas and liquid phases were analyzed by FID-GC. The carbon balance (C.B.) of each analysis result was calculated using eqn (3). The sum of the detected but unidentified products is denoted as “others” in the results. The FID sensitivity of “others” was assumed to be the same as that of 1,4-butanediol. When the C.B. is in the range of $100 \pm 10\%$ considering the experimental error, the conversion and selectivity on the carbon basis are calculated using eqn (4) and (5), respectively, and the data of C.B. are not shown in each result. In contrast, when the C.B. is clearly lower than 100% ($<90\%$), the conversion is calculated using eqn (6). The selectivity to “others” is the same as the above case. The data of C.B. are shown in each result when clearly below 100%. The yield was calculated using eqn (7) and (8) for normal cases and cases with low C.B., respectively. The TOF was calculated using eqn (9) with the increase of conversion ($\Delta\text{conversion}$) from that at 0 h reaction because the reaction proceeded significantly during heating.

$$\text{C. B. (\%)} = \frac{\text{Amount of remaining substrate (C-mol)} + \text{Total amount of detected products (C-mol)}}{\text{Amount of remaining substrate (C-mol)}} \times 100 \quad (3)$$

$$\text{Conversion (\%)} = \frac{\text{Total amount of detected products (C-mol)}}{\text{Amount of remaining substrate (C-mol)} + \text{Total amount of detected products (C-mol)}} \times 100 \quad (4)$$

$$\text{Selectivity to product A (\%)} = \frac{\text{Amount of A (C-mol)}}{\text{Total amount of detected products (C-mol)}} \times 100 \quad (5)$$

$$\text{Conversion (\%; low C. B.)} = 100 - \frac{\text{Amount of remaining substrate (C-mol)}}{\text{Amount of initial substrate (C-mol)}} \times 100 \quad (6)$$

$$\text{Yield (\%)} = \frac{\text{Amount of A (C-mol)} \times 100}{\text{Amount of initial substrate (C-mol)}} = \frac{\text{Conversion (\%)} \times \text{Selectivity (\%)}}{100} \quad (7)$$

$$\text{Yield (\%; low C. B.)} = \frac{\text{Amount of A (C-mol)} \times 100}{\text{Amount of initial substrate (C-mol)}} = \frac{(\text{Conversion (\%)} + \text{C. B. (\%)} - 100) \times \text{Selectivity (\%)}}{100} \quad (8)$$

$$\text{TOF}_{\text{Re-total}} (\text{h}^{-1}) = \frac{\text{Amount of initial substrate (mol)} \times \Delta \text{Conversion (\%)} / 100}{\text{Amount of Re (mol)} \times \Delta \text{Reaction time (h)}} \quad (9)$$

For reuse tests, the catalyst mixture was collected by filtration, washed with 1,4-dioxane and dried for 12 h. The dried catalyst was used directly or after calcination for the next activity test. The calcination conditions were described in each result. The weight loss during the recovery and drying process was about 20%. Typically, multiple runs were carried out simultaneously to collect a sufficient amount of catalyst for the next use, and the number of runs was decreased during reuses (1st use: 4 runs; 2nd use: 3 runs, and so on).

The BET surface area was measured with a Micromeritics Gemini instrument. XRD patterns were obtained with a Rigaku MiniFlex600 diffractometer. H_2 -TPR profiles were obtained with a home-made apparatus equipped with a fixed-bed quartz reactor, frozen acetone trap and TCD. The sample weight was about 50 mg, and the sample was reduced with 5% H_2 in Ar from room temperature to 1173 K at a heating rate of 10 K min^{-1} . Temperature-programmed desorption of NH_3 (NH_3 -TPD) profiles were obtained with a MicrotracBEL BELCAT-II instrument. The sample (50 mg) was first treated with He at 773 K for 1 h, and then NH_3/He (5/95) was passed through the sample at 323 K for 30 min. After purging NH_3 with He at 323 K, the sample was heated at 10 K min^{-1} under flowing He. The desorbed NH_3 was analyzed with MS at the $m/z = 16$ signal. XAFS spectra were measured at the BL01B1 station of SPring-8 (Proposal No. 2019A1369). Detectors for Re L_3 -edge spectra were ion chambers filled with $\text{N}_2/\text{Ar} = 85/15$ and $\text{N}_2/\text{Ar} = 50/50$ for I_0 and I , respectively. Analysis of data was performed using the REX2000 ver. 2.6 program to obtain the XANES spectra. TG-DTA profiles were obtained with a Rigaku Thermo Plus EVO-II instrument using a 10 mg sample and $\alpha\text{-Al}_2\text{O}_3$ reference under static air.

Results and discussion

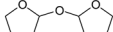
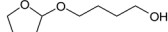
Screening of catalysts

In the one-pot reaction of 1,4-anhydroerythritol (1,4-AHERY) to 1,4-butanediol (1,4-BuD) over the mixed catalyst system of $\text{ReO}_x\text{-Au/CeO}_2$ and ReO_x/C , the ReO_x/C mainly catalyzed the conversion of 2,5-dihydrofuran (2,5-DHF) as an intermediate of 1,4-BuD. Therefore, in order to find a replacement of the ReO_x/C catalyst, we tested various Re catalysts in the reaction of 2,5-DHF (Table 1). One equivalent of water was added to the reaction system based on the stoichiometry, while water was supplied by the first DODH step in the reaction of 1,4-AHERY. Various products were detected including 1,4-BuD, THF, 2,3-dihydrofuran (2,3-DHF) and so on. Among products, γ -butyrolactone (GBL) and addition products of 2,3-DHF (2-hydroxytetrahydrofuran (2-HTHF) and acetals) were regarded as possible precursors of 1,4-BuD because the hydrogenation of these compounds can give 1,4-BuD. Although $\text{ReO}_x/\text{TiO}_2$ was reported to catalyze the conversion of 2,5-DHF to 1,4-BuD in a flow reactor with a co-feed of H_2 and water with 80% yield,⁴² under our reaction conditions, $\text{ReO}_x/\text{TiO}_2$ (entry 2) showed a much lower performance (selectivity to 1,4-BuD and its precursors <40%). Nevertheless, $\text{ReO}_x/\text{TiO}_2$ and $\text{ReO}_x/\text{ZrO}_2$ (entries 2 and 3) showed relatively higher conversion and selectivity to 1,4-BuD than Re catalysts on other oxide supports such as $\text{ReO}_x/\text{Al}_2\text{O}_3$, $\text{ReO}_x/\text{SiO}_2$, $\text{ReO}_x/\text{HZSM5}$, and ReO_x/MgO (entries 4–7). The main products over $\text{ReO}_x/\text{Al}_2\text{O}_3$ and $\text{ReO}_x/\text{HZSM5}$ were THF and furan which are the disproportionation products from DHFs (2,5-DHF and 2,3-DHF; 2DHFs \rightarrow THF + furan). THF was also a main product over $\text{ReO}_x/\text{SiO}_2$ and ReO_x/MgO .

Table 1 Reaction of 2,5-DHF over various Re catalysts^a

Entry	Catalyst	Re loading amount/wt%	Conv./%	Selectivity/%									
				1,4-BuD	THF	2,3-DHF	1-BuOH	GBL	Furan	2-HTHF	Acetal A	Acetal B	Others
1 ^b	ReO _x /C	3	94	60	14	0	2	12	2	0	0	5	5
2	ReO _x /TiO ₂	3	43	21	22	3	18	6	9	2	2	5	11
3	ReO _x /ZrO ₂	3	62	19	20	6	3	17	7	4	1	16	6
4	ReO _x /Al ₂ O ₃	3	23	1	27	11	1	2	26	5	4	1	24
5	ReO _x /SiO ₂	3	25	13	48	11	8	0	9	11	0	0	0
6	ReO _x /HZSM5	3	26	2	45	0	7	0	32	1	0	0	12
7	ReO _x /MgO	3	25	0	35	46	0	0	11	8	0	0	0
8	ReO _x /TiO ₂ -ZrO ₂ ^c	1	57	21	30	10	2	7	4	4	1	17	4
9	ReO _x /SiO ₂ -ZrO ₂ ^d	1	52	22	36	1	3	6	6	2	1	17	2
10	ReO _x /CeO ₂ -ZrO ₂ ^e	1	17	2	37	28	0	0	0	21	0	0	12
11	ReO _x /WO ₃ -ZrO ₂ ^f	1	94	43	38	0	4	5	2	1	0	6	1
12	ReO _x /WO ₃ -ZrO ₂ ^{fg}	1	63	18	39	1	3	10	3	3	0	12	9
13	ReO _x /WO ₃ /TiO ₂ ^h	1	26	3	31	0	5	0	28	5	0	0	27
14	ReO _x /WO ₃ /Al ₂ O ₃ ^h	1	22	9	38	1	2	1	21	10	2	6	9
15	ReO _x /WO ₃ /ZrO ₂ ^h	1	93	40	45	0	5	3	3	0	0	3	1
16	None	—	2	0	38	19	0	0	26	0	11	0	6

^a Reaction conditions: 2,5-DHF = 0.15 g, water = 0.04 g, catalyst = 0.15 g (Re = 1 or 3 wt%), 1,4-dioxane = 4 g, P_{H_2} = 8 MPa, T = 413 K, t = 4 h.

^b Reported in ref. 23. ^c TiO₂ = 30 wt%. ^d SiO₂ = 10 wt%. ^e CeO₂ = 50 wt%. ^f WO₃ = 10 wt%. ^g ReO_x/WO₃-ZrO₂ was reduced in solvent at 413 K for 1 h before the reaction. ^h W = 5 wt%; homemade supports prepared by impregnation. BuD: butanediol, DHF: dihydrofuran, THF: tetrahydrofuran, BuOH: butanol, GBL: γ -butyrolactone, HTHF: hydroxytetrahydrofuran, acetal A: ; acetal B: .

2,3-DHF, which is formed by isomerization of 2,5-DHF, was another main product over ReO_x/MgO, and it was also formed over ReO_x/SiO₂ and ReO_x/Al₂O₃. In the reaction of 2,5-DHF to 1,4-BuD, 2,3-DHF formed by isomerization of 2,5-DHF was next converted by hydration which is typically catalyzed by an acid. The lack of acidity of ReO_x/MgO is related to the high selectivity to 2,3-DHF. In fact, ReO_x/HZSM5 which has high acidity showed 0% selectivity to 2,3-DHF. However, ReO_x/HZSM5 showed little activity in isomerization of 2,5-DHF to 2,3-DHF which was the first step of 1,4-BuD formation. ReO_x/ZrO₂ showed a slightly higher

activity of 2,5-DHF conversion than ReO_x/TiO₂. However, the selectivity to 1,4-BuD over either ReO_x/TiO₂ or ReO_x/ZrO₂ was just around 20%, similar to their selectivity to THF.

All the ReO_x catalysts with a single oxide support showed lower activity and 1,4-BuD selectivity than ReO_x/C (Table 1, entry 1). Therefore, the Re catalysts with mixed oxide supports were further tested in the reaction of 2,5-DHF. Zirconia was selected as one of the components because of the variety of available mixed oxides and relatively good performance of ReO_x/ZrO₂. The ReO_x/WO₃-ZrO₂ catalyst (entry 11) using a commercial WO₃-ZrO₂ support with 10 wt% WO₃

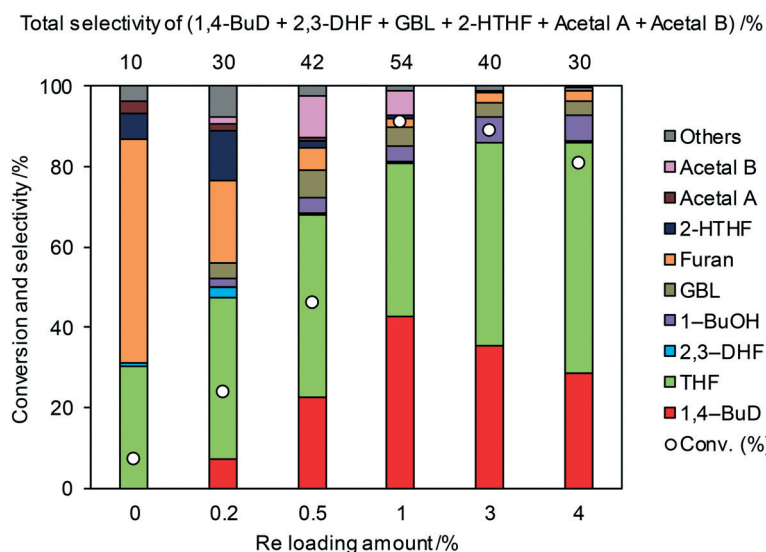
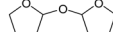
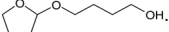


Fig. 1 Effect of Re loading amount of ReO_x/WO₃-ZrO₂ in the reaction of 2,5-DHF. Reaction conditions: 2,5-DHF = 0.15 g, water = 0.04 g, ReO_x/WO₃-ZrO₂ = 0.15 g (Re = 0–4 wt%, WO₃ = 10 wt%), 1,4-dioxane = 4 g, P_{H_2} = 8 MPa, T = 413 K, t = 4 h. DHF: dihydrofuran, BuD: butanediol, THF: tetrahydrofuran, BuOH: butanol, GBL: γ -butyrolactone, HTHF: hydroxytetrahydrofuran, acetal A: ; acetal B: .

loading showed the highest conversion of 2,5-DHF and the highest selectivity to 1,4-BuD among all the catalysts on non-carbon supports. The conversion over $\text{ReO}_x/\text{WO}_3\text{-ZrO}_2$ was as high as that obtained over ReO_x/C , and the selectivity to 1,4-BuD was slightly lower than that of ReO_x/C due to the higher selectivity to THF. Other Re catalysts with mixed oxide supports such as $\text{ReO}_x/\text{TiO}_2\text{-ZrO}_2$, $\text{ReO}_x/\text{SiO}_2\text{-ZrO}_2$, $\text{ReO}_x/\text{CeO}_2\text{-ZrO}_2$, $\text{ReO}_x/\text{WO}_3/\text{TiO}_2$, and $\text{ReO}_x/\text{WO}_3/\text{Al}_2\text{O}_3$ (entries 8–10, 13–14) showed lower activity in the conversion of 2,5-DHF and selectivity to 1,4-BuD than $\text{ReO}_x/\text{WO}_3\text{-ZrO}_2$. The $\text{ReO}_x/\text{WO}_3\text{-ZrO}_2$ catalyst reduced before use (entry 12) showed a lower activity than the non-pretreated one, and the selectivity to 1,4-BuD also decreased, while the selectivity to other intermediates such as 2-hydroxytetrahydrofuran (addition product of 2,3-DHF and water) and acetals increased. This decrease might be due to the aggregation of catalytically active Re sites.

Fig. 1 shows the effect of the Re loading amount of $\text{ReO}_x/\text{WO}_3\text{-ZrO}_2$ in the reaction of 2,5-DHF. Without Re, the conversion was low and the main products were THF and furan which can be produced by disproportionation. More furan was formed than THF, which suggests that some of furan was formed by dehydrogenation of 2,5-DHF. 1,4-BuD was not formed at all over $\text{WO}_3\text{-ZrO}_2$ alone. The conversion and selectivity to 1,4-BuD dramatically increased with the increase of the Re loading amount from 0 to 1 wt%. The optimized Re loading amount was 1 wt% based on the 2,5-DHF conversion and 1,4-BuD selectivity. However, the formation of THF increased when the Re loading amount was over 1 wt%, while the conversion of 2,5-DHF gradually decreased at the same time. The decrease of conversion can be due to the aggregation of catalytically active Re sites to

inactive polymeric Re species (in isomerization of 2,5-DHF to 2,3-DHF). The increase of THF selectivity with the increase of the Re amount can be explained by the hydrogenation ability of polymerized Re species with metallic nature.

Even though 1,4-BuD was formed over the $\text{ReO}_x/\text{ZrO}_2$ catalyst, adding WO_3 to the ZrO_2 support improved the conversion and the selectivity to 1,4-BuD dramatically. In addition to the commercial $\text{WO}_3\text{-ZrO}_2$ (10 wt% WO_3) support, WO_3/ZrO_2 supports with various W amounts were prepared by impregnation and tested as $\text{ReO}_x/\text{WO}_3/\text{ZrO}_2$ catalysts for the reaction of 2,5-DHF (Fig. 2). Up to 5 wt% W, the activity of the $\text{ReO}_x/\text{WO}_3/\text{ZrO}_2$ catalyst increased with increasing W amount. The selectivity to 1,4-BuD and its precursors (acetals and 2-HTHF) became higher when the W amount was between 3 and 5%. The THF formation sharply increased and the selectivity to 1,4-BuD decreased at a higher W loading amount than 5 wt%. The conversion of 2,5-DHF also decreased dramatically when the W loading amount was higher than 5 wt%. In tungsten-zirconia supported Re catalysts, this homemade WO_3/ZrO_2 (W = 5 wt%) support (Table 1, entry 15) showed a similar activity to the commercial $\text{WO}_3\text{-ZrO}_2$ (WO_3 = 10 wt%) support (entry 11). The best W amount in the homemade support (W = 5 wt%) was similar to the W amount of the commercial support (WO_3 = 10 wt%; W = 7.9 wt%) based on the surface area (ZrO_2 : $62 \text{ m}^2 \text{ g}^{-1}$; $\text{WO}_3\text{-ZrO}_2$: $103 \text{ m}^2 \text{ g}^{-1}$). We also prepared a tungsten-zirconia support by co-precipitation ($^{\text{cp}}\text{WO}_3\text{-ZrO}_2$), because the tungsten-zirconia prepared by co-precipitation is known to have a tetragonal ZrO_2 structure⁴³ while pure standard ZrO_2 has the monoclinic phase. The activity of $\text{ReO}_x/^{\text{cp}}\text{WO}_3\text{-ZrO}_2$ (W = 5 wt%) was lower than those of $\text{ReO}_x/\text{WO}_3\text{-ZrO}_2$ (WO_3 = 10 wt%) with a commercial support and

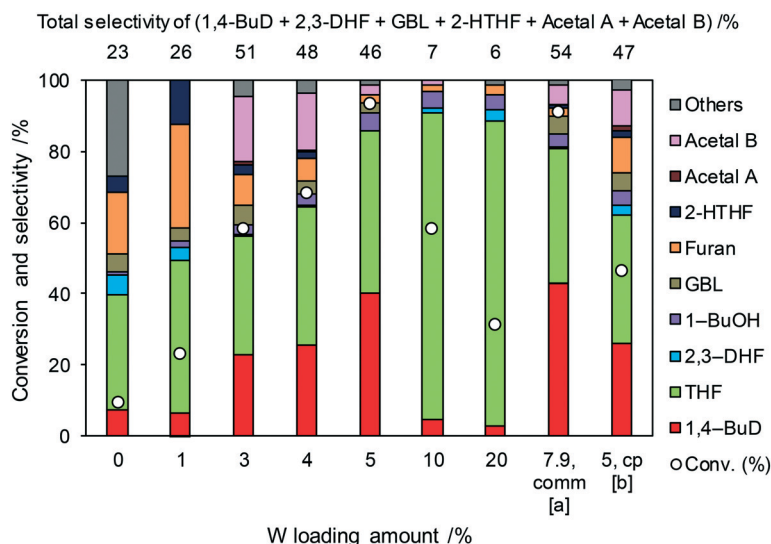


Fig. 2 Effect of W loading amount of $\text{ReO}_x/^{\text{imp}}\text{WO}_3/\text{ZrO}_2$ in the reaction of 2,5-DHF. Reaction conditions: 2,5-DHF = 0.15 g, water = 0.04 g, $\text{ReO}_x/^{\text{imp}}\text{WO}_3/\text{ZrO}_2$ = 0.15 g (Re = 1 wt%, W = 1–20 wt%), 1,4-dioxane = 4 g, P_{H_2} = 8 MPa, T = 413 K, t = 4 h. [a] $\text{ReO}_x/\text{WO}_3\text{-ZrO}_2$ (Re = 1 wt%, WO_3 = 10 wt% (W 7.9 wt%), commercial support). [b] $\text{ReO}_x/^{\text{cp}}\text{WO}_3\text{-ZrO}_2$ (Re = 1 wt%, W = 5 wt%, support prepared by co-precipitation). DHF: dihydrofuran, BuD: butanediol, THF: tetrahydrofuran, BuOH: butanol, GBL: γ -butyrolactone, HTHF: hydroxytetrahydrofuran, acetal A: C1COCC1; acetal B: C1COCCOCC1, com: commercial (WO_3 = 10 wt%).

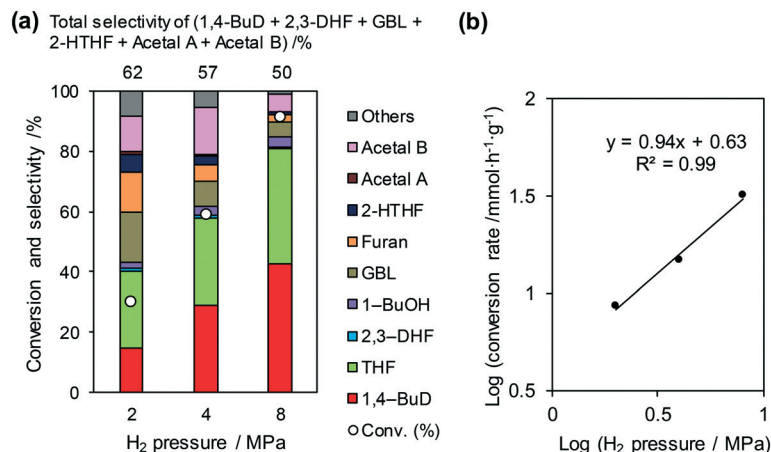
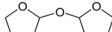
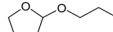


Fig. 3 Effect of H₂ pressure in the reaction of 2,5-DHF over ReO_x/WO₃-ZrO₂. (a) Results at 4 h; (b) initial conversion rate. Reaction conditions: 2,5-DHF = 0.15 g, water = 0.04 g, ReO_x/WO₃-ZrO₂ = 0.15 g (Re = 1 wt%, WO₃ = 10 wt%), 1,4-dioxane = 4 g, P_{H_2} = 2–8 MPa, T = 413 K, t = 4 h (a), 0–2 h (b). The detailed data of (b) are shown in Table S1, ESI†. DHF: dihydrofuran, BuD: butanediol, THF: tetrahydrofuran, BuOH: butanol, GBL: γ -butyrolactone, HTHF: hydroxytetrahydrofuran, acetal A: ; acetal B: .

ReO_x/WO₃/ZrO₂ with the same W amount (5 wt%). We used the commercial WO₃-ZrO₂ (WO₃ = 10 wt%) support in the following studies due to the convenience of accessibility, unless noted. The structure–performance relationship will be discussed in a later section based on the characterization data of various tungsten–zirconia supports.

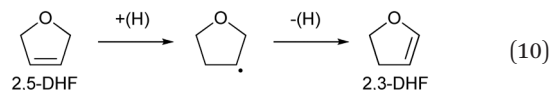
Optimization of reaction conditions

The reaction temperature for the conversion of 2,5-DHF over ReO_x/WO₃-ZrO₂ was optimized to 413 K based on the yield of 1,4-BuD (Fig. S1, ESI†). The conversion and selectivity to 1,4-BuD increased with raising the reaction temperature from 393 to 413 K. The selectivity to 1,4-BuD sharply decreased when the temperature was over 413 K; meanwhile the selectivity to THF dramatically increased probably due to the dehydration of 1,4-BuD.

Fig. 3 shows the effect of H₂ pressure in the reaction of 2,5-DHF over ReO_x/WO₃-ZrO₂ (the detailed data for the reaction rate determination are shown in Fig. S2 and Table S1, ESI†). The conversion and selectivity to 1,4-BuD increased with the increase in hydrogen pressure from 2 to 8 MPa (Fig. 3(a)). Although the THF selectivity increased at the same time, the reaction rate was much higher under 8 MPa hydrogen pressure. The total selectivity to 1,4-BuD + acetals + 2-HTHF + γ -butyrolactone (GBL) as 1,4-BuD and its precursors was similar to the sum of selectivity to furan + THF under different H₂ pressures, even though the 1,4-BuD selectivity was lower and the GBL selectivity was higher under lower H₂ pressure. Therefore, GBL may be an intermediate of 1,4-BuD like 2-HTHF and acetals in the conversion of 2,5-DHF.

The reaction rate dependence on H₂ pressure was also determined based on the reaction results at low conversion levels. The reaction rate of 2,5-DHF increased with increasing H₂ pressure over ReO_x/WO₃-ZrO₂. The reaction order with respect to hydrogen pressure was 0.94 (Fig. 3(b)), indicating

that the rate-determination step was a reaction involving hydrogen species. Although the conversion of 2,5-DHF to 2,3-DHF does not consume hydrogen, the conversion can proceed by addition of a hydrogen atom to the 4-position of 2,5-DHF and removal of a hydrogen atom at the 2 position (eqn (10)). The rate-determining step might be the activation of H₂ or the addition of hydrogen species to the substrate.



As above, the optimized reaction conditions for 1,4-BuD production from 2,5-DHF were a temperature of 413 K and a H₂ pressure of 8 MPa, which were the same reaction conditions used in the reaction of 1,4-AHRY over the combination of ReO_x-Au/CeO₂ (or ReO_x/CeO₂) and ReO_x/C catalysts as reported in our previous reports.^{23,39}

The optimized ReO_x/WO₃-ZrO₂ catalyst was applied to the reaction of 1,4-AHRY combined with the ReO_x-Au/CeO₂ catalyst for DODH of 1,4-AHRY to 2,5-DHF under the standard reaction conditions. The time course of the reaction of 1,4-AHRY over the mixture of ReO_x-Au/CeO₂ and ReO_x/WO₃-ZrO₂ is shown in Fig. 4 (the detailed data are shown in Table S2, ESI†). The selectivity to 1,4-BuD and THF increased with the increase of conversion. At the beginning of the reaction, 2,5-DHF as an intermediate and the acetal from 4-hydroxybutanal and 1,4-AHRY were detected, and they were gradually converted with time. Unlike the time course of 1,4-AHRY reduction over the combination of ReO_x-Au/CeO₂ and ReO_x/C where only the acetal was detected as the main intermediate,²³ 2,5-DHF as an intermediate was detected in a significant amount at a shorter reaction time. This difference means the lower activity of the ReO_x/WO₃-ZrO₂ catalyst in the isomerization of 2,5-DHF to 2,3-DHF than that of ReO_x/C. These results are somewhat inconsistent with the similar

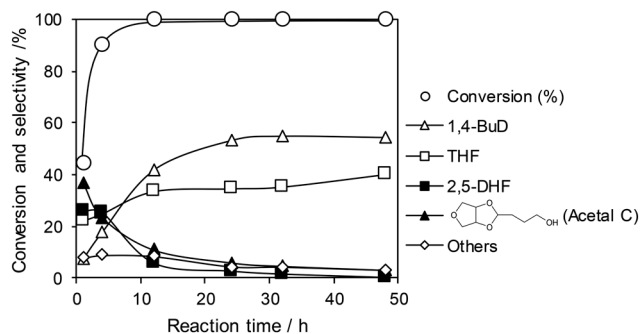


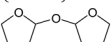
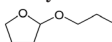
Fig. 4 Time course of the reaction of 1,4-AHERY over $\text{ReO}_x\text{-Au/CeO}_2 + \text{ReO}_x/\text{WO}_3\text{-ZrO}_2$. Reaction conditions: 1,4-AHERY = 0.3 g, $\text{ReO}_x\text{-Au/CeO}_2 = 0.15$ g (Re = 1 wt%, Au = 0.3 wt%), $\text{ReO}_x/\text{WO}_3\text{-ZrO}_2 = 0.15$ g (Re = 1 wt%, $\text{WO}_3 = 10$ wt%), 1,4-dioxane = 4 g, $P_{\text{H}_2} = 8$ MPa, $T = 413$ K, $t = 1\text{--}48$ h. The detailed data are shown in Table S2, ESI†. AHERY: anhydroerythritol, BuD: butanediol, THF: tetrahydrofuran, DHF: dihydrofuran.

activity of $\text{ReO}_x/\text{WO}_3\text{-ZrO}_2$ alone to the ReO_x/C catalyst alone in 2,5-DHF reduction (Table 1, entries 1 and 11). The difference can be explained by the movement of Re species from $\text{WO}_3\text{-ZrO}_2$ to the CeO_2 support as described below. The DHFs were quickly converted over the ReO_x/C catalyst, and the rate-determining step of the $\text{ReO}_x\text{(-Au)/CeO}_2 + \text{ReO}_x/\text{C}$ system for 1,4-AHERY reduction was the DODH catalyzed by $\text{ReO}_x\text{(-Au)/CeO}_2$. In the system of $\text{ReO}_x\text{-Au/CeO}_2 + \text{ReO}_x/\text{WO}_3\text{-ZrO}_2$, the rate-determining step in the conversion of 1,4-AHERY was not clear: the DODH step and isomerization step had similar reaction rates. The highest yield of 1,4-BuD was 55% obtained at 32 h, which was significantly lower than the 90% over the co-catalyst of $\text{ReO}_x\text{-Au/CeO}_2$ and ReO_x/C , due to the high selectivity to THF in the reaction. Because

THF was formed from several pathways (DHF hydrogenation, DHF disproportionation, and 1,4-BuD dehydration), the improvement of the 1,4-BuD yield in the reaction of 1,4-AHERY over the mixture catalyst of $\text{ReO}_x\text{-Au/CeO}_2$ and $\text{ReO}_x/\text{WO}_3\text{-ZrO}_2$ might be difficult. The $\text{TOF}_{\text{Re-total}}$ based on the conversion and total Re amount of the mixture of $\text{ReO}_x\text{-Au/CeO}_2 + \text{ReO}_x/\text{WO}_3\text{-ZrO}_2$, which means the $\text{TOF}_{\text{Re-total}}$ of the first DODH step, is calculated to be $3 \times 10 \text{ h}^{-1}$ (conversion of 45% \rightarrow 90% from 1 to 4 h, Fig. 4 and Table S2†). Although this value could have considerable error because of the limited data points and high conversion levels, this value is comparable to the $\text{TOF}_{\text{Re-total}}$ of $\text{CeO}_2 + \text{ReO}_x/\text{C}$ (Re 2 wt%) in 1,4-AHERY reduction to 1,4-BuD (26 h^{-1})³⁹ at the same temperature and H_2 pressure. According to our previous works in DODH using $\text{ReO}_x/\text{CeO}_2 + \text{promoter}$ catalysts, the DODH activity is controlled by the amount of monomeric ReO_x species on CeO_2 , while Re species on C and other oxide supports are inactive in DODH.³⁹ Therefore, the $\text{TOF}_{\text{Re-total}}$ value of mixture catalysts is reflected by the ratio of the Re amount on CeO_2 to the total Re amount. It was reported that $\text{ReO}_x\text{-Au/CeO}_2$ (1 wt%) + ReO_x/C (3 wt%) showed a much lower $\text{TOF}_{\text{Re-total}}$ (5 h^{-1}) because the number of active Re sites on CeO_2 for DODH is fixed by the rapid reduction of both Re species on CeO_2 and C to insoluble species. In the case of $\text{CeO}_2 + \text{ReO}_x/\text{C}$, the Re species move from the C support to the CeO_2 support before reduction to form a large number of active Re sites for DODH. The similar high $\text{TOF}_{\text{Re-total}}$ value of $\text{ReO}_x\text{-Au/CeO}_2 + \text{ReO}_x/\text{WO}_3\text{-ZrO}_2$ to that of $\text{CeO}_2 + \text{ReO}_x/\text{C}$ suggests that some of the Re species on $\text{WO}_3\text{-ZrO}_2$ moved to the CeO_2 support. On the other hand, the decrease of the Re amount in $\text{ReO}_x/\text{WO}_3\text{-ZrO}_2$ would lower the activity in 2,5-DHF conversion when it was mixed with $\text{ReO}_x\text{-Au/CeO}_2$.

Table 2 Reaction of 1,4-AHERY and the intermediates over related catalysts^a

Entry	Substrate	Catalyst	Conv./% (C. B./%)	Selectivity/%										Acetal		Others
				1,4-BuD	THF	2,5-DHF	2,3-DHF	1-BuOH	GBL	Furan	2-HTHF	A	B			
1	1,4-AHERY	$\text{ReO}_x\text{-Au/CeO}_2 + \text{ReO}_x/\text{WO}_3\text{-ZrO}_2$	100	53	35	3	0	2	1	0	0	0	1	6		
2		$\text{ReO}_x/\text{CeO}_2 + \text{ReO}_x/\text{WO}_3\text{-ZrO}_2$	1	0	0	64	0	0	0	0	0	0	0	36		
3 ^{b,c}		$\text{ReO}_x\text{-Au/CeO}_2$	64	0	1	89	5	0	0	0	1	0	0	3		
4		$\text{ReO}_x/\text{WO}_3\text{-ZrO}_2$	1	0	0	0	0	0	63	0	0	0	0	37		
5 ^{b,d}	2,5-DHF	$\text{ReO}_x\text{-Au/CeO}_2$	45	4	34	—	54	2	0	2	2	0	0	1		
6 ^d		$\text{ReO}_x/\text{WO}_3\text{-ZrO}_2$	94	43	38	—	0	4	5	2	1	0	6	1		
7 ^d		$\text{WO}_3\text{-ZrO}_2$	7	0	30	—	1	0	0	56	7	3	0	3		
8 ^d		ZrO_2	5	0	36	—	5	1	4	29	8	2	0	16		
9 ^d		None	2	0	38	—	19	0	0	26	0	11	0	6		
10 ^{b,e}	2,3-DHF	$\text{ReO}_x\text{-Au/CeO}_2$ ^b	49 (71)	8	6	0	—	0	3	2	41	23	2	13		
11 ^e		$\text{ReO}_x/\text{WO}_3\text{-ZrO}_2$	100 (20)	32	6	0	—	0	15	0	3	0	15	30		
12 ^e		$\text{WO}_3\text{-ZrO}_2$	98 (21)	9	6	0	—	0	21	0	18	5	18	23		
13 ^e		ZrO_2	76 (62)	4	0	0	—	0	12	0	30	18	16	19		
14 ^{e,f}		MgO	32 (79)	0	0	3	—	0	5	0	64	23	0	6		
15 ^e		None	27 (80)	0	0	0	—	0	0	4	76	10	0	10		

^a Reaction conditions: 1,4-AHERY = 0.3 g, catalyst = 0.15 g (or 0.15 g + 0.15 g), 1,4-dioxane = 4 g, $P_{\text{H}_2} = 8$ MPa, $T = 413$ K, $t = 24$ h. ^b Reported in ref. 23. ^c 1,4-AHERY = 0.5 g. ^d 2,5-DHF = 0.15 g, water 0.04 g, $t = 4$ h. ^e 2,3-DHF = 0.15 g, water 0.04 g, $t = 4$ h. ^f $\text{MgO} = 0.15$ g. C. B.: carbon balance; only described when it was clearly different from 100% ($\pm 10\%$). AHERY: anhydroerythritol, BuD: butanediol, THF: tetrahydrofuran, DHF: dihydrofuran, BuOH: butanol, GBL: γ -butyrolactone, acetal A: , acetal B: .

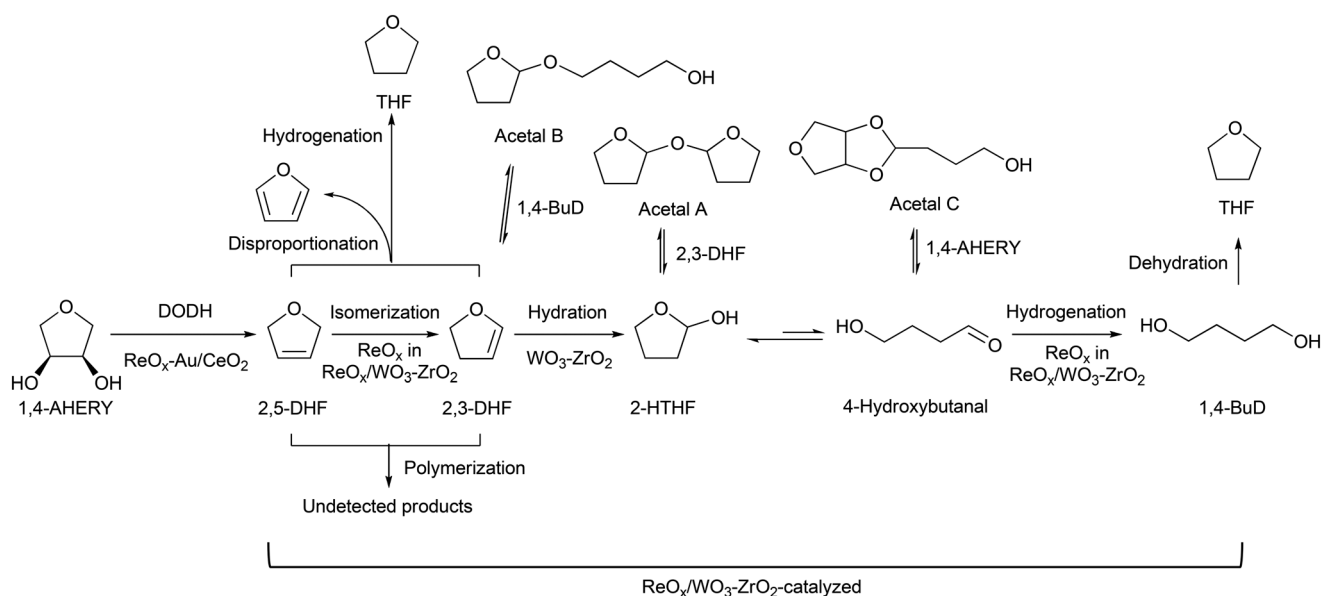
Reaction mechanism

As described above, 1,4-BuD could be produced from 1,4-AHery over the physical mixture of $\text{ReO}_x\text{-Au/CeO}_2$ and $\text{ReO}_x/\text{WO}_3\text{-ZrO}_2$ catalysts (Table 2, entry 1). However, the combination of $\text{ReO}_x/\text{CeO}_2$ and $\text{ReO}_x/\text{WO}_3\text{-ZrO}_2$ showed very low activity in the conversion of 1,4-AHery (entry 2). This indicates that the Au promoter is necessary for the activation of H_2 in the DODH reaction of 1,4-AHery to 2,5-DHF, because the single $\text{ReO}_x/\text{WO}_3\text{-ZrO}_2$ catalyst also showed very low activity to 1,4-AHery conversion (entry 4). Unlike the mechanism of the mixed catalyst of $\text{ReO}_x/\text{CeO}_2$ and ReO_x/C , the Re species on CeO_2 could not be reduced by hydrogen species activated on the $\text{ReO}_x/\text{WO}_3\text{-ZrO}_2$ support. The difference between C and $\text{WO}_3\text{-ZrO}_2$ supports as the promoting ability of $\text{ReO}_x/\text{CeO}_2$ reduction may be related to the electrical conductivity: the C support can more easily transport electrons, which are produced from H_2 along with H^+ , than the oxide support. Therefore, the DODH reaction of 1,4-AHery to 2,5-DHF was entirely catalyzed by $\text{ReO}_x\text{-Au/CeO}_2$. However, the conversion of 1,4-AHery over $\text{ReO}_x\text{-Au/CeO}_2 + \text{ReO}_x/\text{WO}_3\text{-ZrO}_2$ (entry 1) was higher than that over $\text{ReO}_x\text{-Au/CeO}_2$ (entry 3). The increase can be explained by the movement of Re species from $\text{WO}_3\text{-ZrO}_2$ to CeO_2 as explained in the above section.

In the conversion of 2,5-DHF, single $\text{WO}_3\text{-ZrO}_2$ (Table 2, entry 7) or ZrO_2 (entry 8) without Re loading showed very low activity, and the main products were THF and furan, which were co-produced by disproportionation of DHFs. Generally, furan is easily hydrogenated to THF over a metal catalyst and H_2 ; therefore, furan is an unfavorable by-product. The higher THF selectivity of $\text{ReO}_x/\text{WO}_3\text{-ZrO}_2$ was due to the activity of the $\text{WO}_3\text{-ZrO}_2$ support in disproportionation of 2,5-DHF to some extent. However, the yield of THF over $\text{ReO}_x/\text{WO}_3\text{-ZrO}_2$

(entry 6) was higher than that of THF + furan over $\text{WO}_3\text{-ZrO}_2$ (entry 8), suggesting that another route existed for THF formation such as hydrogenation of DHFs. The formation of 2,3-DHF and 1,4-BuD was negligible over the $\text{WO}_3\text{-ZrO}_2$ support without Re, indicating that the Re species have the function of catalyzing the conversion of 2,5-DHF to 2,3-DHF which was the first step in the production of 1,4-BuD from 2,5-DHF. Although $\text{ReO}_x\text{-Au/CeO}_2$ could catalyze a part of the conversion of 2,5-DHF to 2,3-DHF (entry 5), it is difficult to catalyze the hydration of 2,3-DHF to 2-HTHF. The total yield of 1,4-BuD and its precursors over $\text{ReO}_x/\text{WO}_3\text{-ZrO}_2$ was higher than that over $\text{ReO}_x\text{-Au/CeO}_2$, indicating that the isomerization step of 2,5-DHF to 2,3-DHF in 1,4-AHery conversion over $\text{ReO}_x\text{-Au/CeO}_2 + \text{ReO}_x/\text{WO}_3\text{-ZrO}_2$ was mainly catalyzed by the Re species on the $\text{WO}_3\text{-ZrO}_2$ support.

The reaction of 2,3-DHF was investigated next (Table 2, entries 10–15). Similar to the reaction of 2,5-DHF, although $\text{ReO}_x\text{-Au/CeO}_2$ could partially catalyze the hydration of 2,3-DHF to 2-HTHF and the acetals (entry 10), the conversion activity was lower than that of $\text{ReO}_x/\text{WO}_3\text{-ZrO}_2$ (entry 11) or $\text{WO}_3\text{-ZrO}_2$ (entry 12), suggesting that the hydration of 2,3-DHF was mainly catalyzed by $\text{WO}_3\text{-ZrO}_2$. Acidity is probably necessary in the hydration of 2,3-DHF to 2-HTHF and its derivatives. Basic supports such as MgO (entry 14) showed much lower conversion than non-basic supports like ZrO_2 (entry 13) and $\text{WO}_3\text{-ZrO}_2$ (entry 12), and the results were similar to the case without a catalyst (entry 15). Furthermore, the addition of WO_3 to ZrO_2 increased the conversion probably due to the stronger acidity of $\text{WO}_3\text{-ZrO}_2$ than ZrO_2 . The carbon balance over $\text{ReO}_x/\text{WO}_3\text{-ZrO}_2$, $\text{WO}_3\text{-ZrO}_2$, and ZrO_2 (entries 11–13) was low, which might be due to the formation of polymers from 2,3-DHF as well as the evaporation of 2,3-DHF (boiling point: 328 K). A similar low carbon balance in the reaction of 2,3-DHF has been also

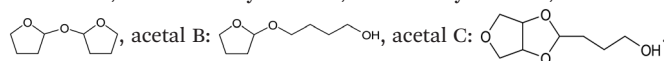


Scheme 2 Reaction routes of 1,4-AHery reduction to 1,4-BuD over $\text{ReO}_x\text{-Au/CeO}_2 + \text{ReO}_x/\text{WO}_3\text{-ZrO}_2$.

Table 3 Reuse of the $\text{ReO}_x\text{-Au/CeO}_2 + \text{ReO}_x/\text{WO}_3\text{-ZrO}_2$ catalyst mixture in the reaction of 1,4-AHERY^a

Entry	Calcination conditions	Usage times	Conv./%	Selectivity/%									
				1,4-BuD	THF	GBL	1-BuOH	2,5-DHF	2,3-DHF	Acetal A	Acetal B	Acetal C	Others
1	—	1	100	53	31	1	2	5	0	0	1	6	0
2 ^b	None	2	97	25	23	4	1	12	2	0	20	8	5
3 ^b	573 K, 1 h	2	100	46	38	0	2	1	0	0	1	11	1
4 ^b	573 K, 1 h	3	84	35	44	0	2	2	0	0	1	13	3
5 ^b	573 K, 3 h	2	100	49	39	0	2	5	0	0	0	4	1
6 ^b	573 K, 3 h	3	100	43	34	1	2	13	1	0	3	2	1
7 ^b	773 K, 3 h	2	80	38	41	0	2	1	1	0	1	14	2
8 ^b	773 K, 3 h	3	68	26	18	6	1	26	1	0	8	6	9
9 ^c	None	2	100	51	35	1	2	0	0	0	1	10	1
10 ^d	None	2	68	32	36	0	2	2	0	0	3	23	2

^a Reaction conditions: 1,4-AHERY = 0.3 g, $\text{ReO}_x\text{-Au/CeO}_2$ = 0.15 g (Re = 1 wt%, Au = 0.3 wt%), $\text{ReO}_x/\text{WO}_3\text{-ZrO}_2$ = 0.15 g (Re = 1 wt%, WO_3 = 10 wt%), 1,4-dioxane = 4 g, P_{H_2} = 8 MPa, T = 413 K, t = 24 h. ^b Recycled $\text{ReO}_x\text{-Au/CeO}_2 + \text{ReO}_x/\text{WO}_3\text{-ZrO}_2$ mixture = 0.3 g. ^c Recycled $\text{ReO}_x\text{-Au/CeO}_2 + \text{ReO}_x/\text{WO}_3\text{-ZrO}_2$ mixture = 0.24 g, and fresh $\text{ReO}_x\text{-Au/CeO}_2$ = 0.06 g (Re = 1 wt%, Au = 0.3 wt%) was added. ^d Recycled $\text{ReO}_x\text{-Au/CeO}_2 + \text{ReO}_x/\text{WO}_3\text{-ZrO}_2$ mixture = 0.24 g, and fresh $\text{ReO}_x/\text{WO}_3\text{-ZrO}_2$ = 0.06 g (Re = 1 wt%, WO_3 = 10 wt%) was added. AHERY: anhydroerythritol, BuD: butanediol, THF: tetrahydrofuran, DHF: dihydrofuran, BuOH: butanol, GBL: γ -butyrolactone, HTHF: hydroxytetrahydrofuran, acetal A:



reported over the ReO_x/C catalyst.²³ The low concentration of 2,3-DHF in the reaction of 1,4-AHERY and the presence of basic $\text{ReO}_x\text{-Au/CeO}_2$ can suppress the loss of carbon balance in the reaction of 1,4-AHERY over $\text{ReO}_x\text{-Au/CeO}_2 + \text{ReO}_x/\text{WO}_3\text{-ZrO}_2$. The selectivity to 1,4-BuD was dramatically increased when the Re species were loaded on $\text{WO}_3\text{-ZrO}_2$. This indicates that the hydrogenation of 2-HTHF-derived products to 1,4-BuD was mainly catalyzed by the Re species on $\text{WO}_3\text{-ZrO}_2$, although the W species in $\text{WO}_3\text{-ZrO}_2$ have some activity in hydrogenation (or transfer hydrogenation) of 2-HTHF-derived products to 1,4-BuD.

Based on these results, we propose a reaction mechanism of 1,4-AHERY to 1,4-BuD over the combination of $\text{ReO}_x\text{-Au/CeO}_2$ and $\text{ReO}_x/\text{WO}_3\text{-ZrO}_2$ (Scheme 2) similar to the one we proposed for the mixture of $\text{ReO}_x\text{-Au/CeO}_2$ and ReO_x/C .^{23,39} It is composed of $\text{ReO}_x\text{-Au/CeO}_2$ -catalyzed DODH of 1,4-AHERY to 2,5-DHF and $\text{ReO}_x/\text{WO}_3\text{-ZrO}_2$ -catalyzed reduction of 2,5-DHF to 1,4-BuD. In the conversion of 2,5-DHF, the Re species of $\text{ReO}_x/\text{WO}_3\text{-ZrO}_2$ firstly catalyzed the isomerization of 2,5-DHF to 2,3-DHF, and then $\text{WO}_3\text{-ZrO}_2$ catalyzed the hydration of 2,3-DHF to 2-HTHF-derivatives; finally the Re species on $\text{ReO}_x/\text{WO}_3\text{-ZrO}_2$ catalyzed the hydrogenation of the 2-HTHF-derived intermediates to 1,4-BuD.

Catalyst stability

We were unable to reuse the mixed catalyst of $\text{ReO}_x\text{-Au/CeO}_2 + \text{ReO}_x/\text{C}$ due to the deactivation after catalytic use, as well as the difficulty in regeneration because of the combustibility of the carbon support,^{23,39} while $\text{ReO}_x\text{-Au/CeO}_2$ for DODH can be totally regenerated by calcination without a change of catalyst structure including the Au particle size.³² Therefore, the reusability of the $\text{ReO}_x/\text{WO}_3\text{-ZrO}_2$ catalyst combined with $\text{ReO}_x\text{-Au/CeO}_2$ was the most important part in this study. Table 3 shows the results of reuse tests of the mixed catalyst

of $\text{ReO}_x\text{-Au/CeO}_2 + \text{ReO}_x/\text{WO}_3\text{-ZrO}_2$ in the reaction of 1,4-AHERY to 1,4-BuD. When the catalyst mixture was reused without treatment, the selectivity to 1,4-BuD of the $\text{ReO}_x\text{-Au/CeO}_2 + \text{ReO}_x/\text{WO}_3\text{-ZrO}_2$ mixture dramatically decreased from 53% in the first run to 25% in the second run, and the conversion also decreased from 100% to 97% (entries 1 and 2). The product composition was similar to the reaction result of half the reaction time (12 h, Fig. 4), indicating that the catalytic activity of $\text{ReO}_x\text{-Au/CeO}_2 + \text{ReO}_x/\text{WO}_3\text{-ZrO}_2$ decreased after the reaction. Due to the oxide support, the $\text{ReO}_x/\text{WO}_3\text{-ZrO}_2$ catalyst could be calcined to remove the deposits on the catalyst surface. According to the TG-DTA profile of the $\text{ReO}_x\text{-Au/CeO}_2 + \text{ReO}_x/\text{WO}_3\text{-ZrO}_2$ mixture after use (Fig. S3, ESI†), the deposits on the catalyst surface could be removed in the calcination temperature range from 450 K

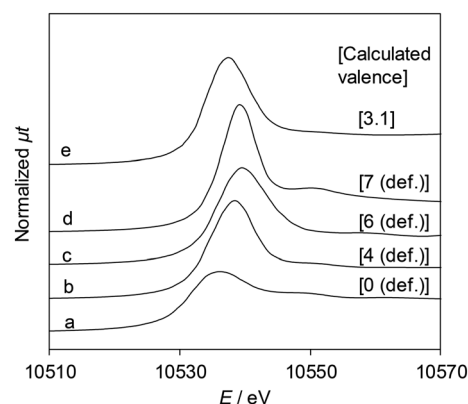


Fig. 5 Re L_3 -edge XANES spectra and the Re valence calculated using the white line area. (a) Re powder, (b) ReO_2 , (c) ReO_3 , (d) Re_2O_7 , and (e) $\text{ReO}_x/\text{WO}_3\text{-ZrO}_2$ after the reaction (reaction conditions: 2,5-DHF 0.15 g, water 0.03 g, catalyst 0.15 g, 1,4-dioxane 4 g, H_2 8 MPa, 413 K, 4 h). The relationship between the white line area and Re valence is shown in Table S4 and Fig. S4, ESI†.

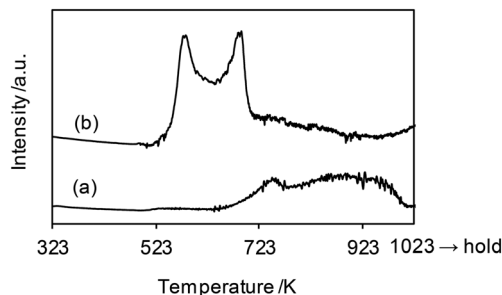


Fig. 6 H_2 -TPR profiles of (a) $\text{WO}_3\text{-ZrO}_2$ (WO_3 = 10 wt%) and (b) $\text{ReO}_x/\text{WO}_3\text{-ZrO}_2$ (Re = 1 wt%, WO_3 = 10 wt%). Measurement conditions: sample weight 50 mg, H_2/Ar = 5/95, 10 K min^{-1} . The H_2 consumption amount is summarized in Table 4.

to 650 K. Therefore, the calcination temperature was set at 573 K (entries 3–6) or 773 K (entries 7 and 8). The best results were obtained with the calcination at 573 K for a longer time (3 h; entries 5 and 6). The conversion and selectivity to 1,4-BuD were almost the same in the reaction of 1,4-AHery over the recycled catalyst mixture of $\text{ReO}_x\text{-Au/CeO}_2 + \text{ReO}_x/\text{WO}_3\text{-ZrO}_2$ calcined at 573 K for 1 or 3 h in the second run (entries 3 and 5, respectively). However, the conversion of 1,4-AHery obviously dropped in the third run over the recycled catalyst mixture calcined at 573 K for 1 h, and the selectivity to 1,4-BuD also decreased with increasing THF selectivity (entry 4). On the other hand, the conversion was still 100% in the third run over the recycled catalyst mixture calcined at 573 K for 3 h, and the selectivity to 1,4-BuD was similar to that of the fresh one (entry 6). Therefore, the co-catalyst system of $\text{ReO}_x\text{-Au/CeO}_2 + \text{ReO}_x/\text{WO}_3\text{-ZrO}_2$ showed potential to be reused by calcination at 573 K for 3 h to regenerate the catalytic activity. The conversion and 1,4-BuD selectivity sharply decreased in the reuse tests over the recycled catalyst mixture calcined at the higher temperature of 773 K for 3 h (entries 7 and 8), indicating that the higher calcination temperature also caused the deactivation of the catalyst mixture. The replenishment of the fresh $\text{ReO}_x\text{-Au/CeO}_2$ catalyst to the recycled mixture of $\text{ReO}_x\text{-Au/CeO}_2 + \text{ReO}_x/\text{WO}_3\text{-ZrO}_2$ without calcination could recover the activity to the fresh level (entry 9). On the other hand, the replenishment of fresh $\text{ReO}_x/\text{WO}_3\text{-ZrO}_2$ to the used catalyst mixture showed the conversion of 1,4-AHery at almost the expected level by the decreased amount of $\text{ReO}_x\text{-Au/CeO}_2$ (ca. 20% weight loss during the collection; conversion decreased by about 30%) (entry 10). These results demonstrated that the decrease of performance was mainly caused by the deactivation of the $\text{ReO}_x\text{-Au/CeO}_2$ catalyst.

Characterization

Fig. 5 shows the Re L_3 -edge XANES spectra of $\text{ReO}_x/\text{WO}_3\text{-ZrO}_2$ and reference compounds. The detailed linear relationship between white line areas and average valence⁴⁴ is shown in Table S4 and Fig. S4, ESI.† The average Re valence of $\text{ReO}_x/\text{WO}_3\text{-ZrO}_2$ after use in 2,5-DHF reduction was +3.1. On the other hand, $\text{ReO}_x/\text{WO}_3\text{-ZrO}_2$ showed activity in hydrogenation of 4-hydroxybutanal to 1,4-BuD, suggesting that some of the Re species were reduced to the metallic state. We have reported that the Re/SiO_2 catalyst with a similar average Re valence (2.6) determined by the same XANES method contains Re^0 sites interacting with Re^{n+} , and the Re/SiO_2 catalyst has activity in carboxylic acid hydrogenation.⁴⁵

The H_2 -TPR profiles of $\text{WO}_3\text{-ZrO}_2$ and $\text{ReO}_x/\text{WO}_3\text{-ZrO}_2$ are shown in Fig. 6, and Table 4 summarizes the H_2 consumption amount in H_2 -TPR. $\text{WO}_3\text{-ZrO}_2$ showed a broad signal at 623–1000 K, which can be assigned to the reduction of WO_3 in $\text{WO}_3\text{-ZrO}_2$. The H_2 consumption of this broad signal was 0.0082 mmol (50 mg sample), which corresponded to the valence change of W by 0.74. On the other hand, $\text{ReO}_x/\text{WO}_3\text{-ZrO}_2$ had strong two bands in the range 500–723 K and a broad band up to 923 K. The broad reduction signal of W was shifted from that in the case without ReO_x to lower temperature, probably by the supply of hydrogen species activated on the reduced Re site. We assume that the band for W reduction with the same H_2 consumption amount (0.0082 mmol) as $\text{WO}_3\text{-ZrO}_2$ was overlapped with Re reduction bands. With this assumption, the H_2 consumption for W reduction in $\text{ReO}_x/\text{WO}_3\text{-ZrO}_2$ between 500 and 723 K was estimated to be 0.0032 mmol (= 0.0082–0.0050 mmol), and the H_2 consumption amount for Re reduction was calculated to be 0.0052 mmol (= 0.084–0.0032 mmol). This consumption amount corresponds to the Re valence change from +7 to +3.1, which agreed well with the XANES results. Although the temperature range of this signal (500–723 K) was higher than the reaction temperature (413 K), the reduction of Re species could take place in the reaction temperature due to the higher H_2 pressure.⁴⁵ Considering the higher temperature range and small H_2 consumption amount for the reduction of W, only a small portion of W species in $\text{ReO}_x/\text{WO}_3\text{-ZrO}_2$ was probably reduced to the +5 valence state during the catalysis, while most of the W species retained the +6 valence state.

An NH_3 -TPD experiment was carried out to determine the acidity of catalysts. The NH_3 -TPD profiles of $\text{WO}_3\text{-ZrO}_2$, carbon and Re catalysts on these supports are shown in Fig. S5, ESI.† The desorbed NH_3 amount from $\text{WO}_3\text{-ZrO}_2$ was

Table 4 Summary of TPR results (Fig. 6)

Sample	Sample weight/mg	Re amount/mmol	W amount/mmol	H_2 consumption amount/mmol (temperature range/K)
(a) $\text{WO}_3\text{-ZrO}_2$	50	—	0.022	0.0082 (500–1000)
(b) $\text{ReO}_x/\text{WO}_3\text{-ZrO}_2$	50	0.0027	0.022	0.0084 (500–723) 0.0050 (723–923)

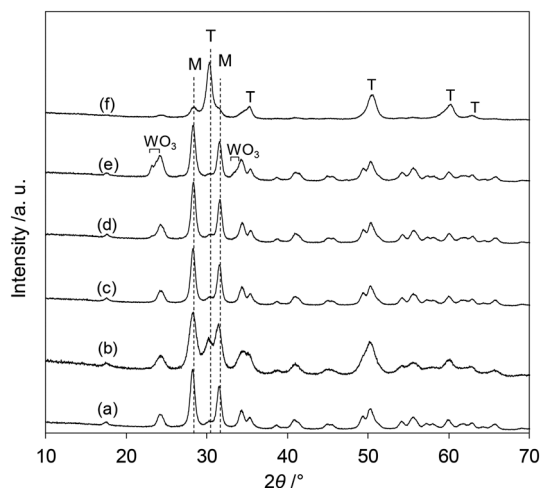


Fig. 7 XRD patterns of tungsten-zirconia-supported Re catalysts after calcination. (a) $\text{ReO}_x/\text{ZrO}_2$ (Re = 3 wt%), (b) $\text{ReO}_x/\text{WO}_3\text{-ZrO}_2$ (Re = 1 wt%, WO_3 = 10 wt%, commercial support), (c) $\text{ReO}_x/\text{WO}_3/\text{ZrO}_2$ (Re = 1 wt%, W = 5 wt%), (d) $\text{ReO}_x/\text{WO}_3/\text{ZrO}_2$ (Re = 1 wt%, W = 10 wt%), (e) $\text{ReO}_x/\text{WO}_3/\text{ZrO}_2$ (Re = 1 wt%, W = 20 wt%), and (f) $\text{ReO}_x/\text{c}^\text{p}\text{WO}_3\text{-ZrO}_2$ (Re = 1 wt%, W = 5 wt%; $\text{WO}_3\text{-ZrO}_2$ was prepared by the co-precipitation method). T: tetragonal ZrO_2 , M: monoclinic ZrO_2 .

larger than that from the carbon support, indicating that the acidity of $\text{WO}_3\text{-ZrO}_2$ is stronger than that of carbon. However, the performance of ReO_x/C combined with $\text{ReO}_x\text{-Au/CeO}_2$ in the reaction of 1,4-AHRY is much higher than that of $\text{ReO}_x/\text{WO}_3\text{-ZrO}_2$. As mentioned above, while acidity is probably necessary in the hydration of 2,3-DHF to 2-HTHF-derivatives, it might not be a significant factor on the overall reaction of 1,4-AHRY to 1,4-BuD since DODH of 1,4-AHRY and 2,5-DHF isomerization to 2,3-DHF are slower steps than hydration of 2,3-DHF. In addition, mixing a basic material (CeO_2 in $\text{ReO}_x\text{-Au/CeO}_2$) with $\text{ReO}_x/\text{WO}_3\text{-ZrO}_2$ in the reaction media can affect the acidity. Also considering the low carbon balance in the reaction tests of 2,3-DHF (Table 2), we do not give a decisive conclusion for the acidity-performance relationship from these $\text{NH}_3\text{-TPR}$ data.

The XRD patterns of the tungsten-zirconia-supported Re catalysts are shown in Fig. 7. The Re species did not show peaks due to the low loading amount and/or low crystallinity on the support surface for all the catalysts. The catalyst with commercial $\text{WO}_3\text{-ZrO}_2$ which has been mainly used as a support in this study (Fig. 7(b)) had mainly a monoclinic structure of ZrO_2 (characteristic peaks at around 28 and 32°) and a small amount of tetragonal ZrO_2 structure (characteristic peak at 30°). In order to determine which phase is more active, the crystalline structures of the series of catalysts with home-made supports were determined and the catalytic performances were correlated with the structures. The commercial ZrO_2 had a monoclinic crystalline structure (Fig. 7(a)). WO_3/ZrO_2 prepared by impregnation of ZrO_2 showed also a monoclinic ZrO_2 structure while there were small peaks of WO_3 when the loading of W was high (≥ 10 wt%) (Fig. 7(c-e)). The ZrO_2 of $\text{c}^\text{p}\text{WO}_3\text{-ZrO}_2$ prepared by the co-precipitation method formed a tetragonal crystalline

structure (t-ZrO_2) (Fig. 7(f)), as reported in the literature.⁴³ As shown in Fig. 1, all the $\text{ReO}_x/\text{tungsten-zirconia}$ catalysts except $\text{ReO}_x/\text{WO}_3/\text{ZrO}_2$ with high W loading (≥ 10 wt%) showed activity in 2,5-DHF reduction to 1,4-BuD. The activity difference can be simply explained by the surface concentration of W species, because $\text{WO}_3\text{-ZrO}_2$ prepared by impregnation should have a higher surface concentration of W than $\text{c}^\text{p}\text{WO}_3\text{-ZrO}_2$ prepared by co-precipitation with a similar surface area (actual surface area of supports: 62 and 68 $\text{m}^2 \text{g}^{-1}$, respectively) and the same W amount (5 wt%). The performance of $\text{ReO}_x/\text{c}^\text{p}\text{WO}_3\text{-ZrO}_2$ corresponded to that of $\text{ReO}_x/\text{WO}_3/\text{ZrO}_2$ with 2–3 wt% W loading. Therefore, the crystalline structure of ZrO_2 does not have a critical role in the catalysts. On the other hand, $\text{ReO}_x/\text{WO}_3/\text{ZrO}_2$ with high W loading had very low activity (Fig. 2). The presence of WO_3 crystallites seemed to deactivate the Re species. The similar crystal structure of WO_3 and ReO_3 (partially reduced rhenium oxide) might be related to the low activity, by incorporation of Re species into the WO_3 crystal. In the literature, WO_3 species on ZrO_2 with lower loading can form monolayer or sub-monolayer species composed of a two-dimensional plane of corner-shared WO_6 octahedra,⁴⁶ and the loading amount per surface area (5 wt% on 62 $\text{m}^2 \text{g}^{-1}$ support; 2.7 W atoms per nm^2) was slightly lower than the monolayer coverage (5 W atoms per nm^2).⁴⁷ The similar catalytic performance of $\text{ReO}_x/\text{WO}_3\text{-ZrO}_2$ (commercial) to $\text{ReO}_x/\text{WO}_3/\text{ZrO}_2$ (5 wt% W) and similar W loading amount per surface area (7.9 wt% in 103 $\text{m}^2 \text{g}^{-1}$ $\text{WO}_3\text{-ZrO}_2$) suggest that the good catalytic performance of $\text{ReO}_x/\text{WO}_3\text{-ZrO}_2$ is also derived from surface submonolayer WO_3 on ZrO_2 . Also considering the similar structure of WO_3 and ReO_3 , Re species during reduction can spread over the WO_3 (sub)monolayer and high dispersion of Re species can be obtained. Considering that both 2,5-DHF isomerization and 4-hydroxybutanal hydrogenation, which were catalyzed by the Re species in $\text{ReO}_x/\text{WO}_3\text{-ZrO}_2$, involve hydrogen species, the highly dispersed Re^0 species on the $\text{WO}_3\text{-ZrO}_2$ support can be the active sites for these steps.

Conclusions

In order to solve the problem of the reusability of the mixture of $\text{ReO}_x\text{-Au/CeO}_2$ and carbon-supported Re catalysts to produce 1,4-butanediol (1,4-BuD) from 1,4-anhydroerythritol (1,4-AHRY) in a one-pot reaction, oxide supports were used to replace the combustible carbon support. We found that the tungsten-zirconia-supported Re catalyst combined with $\text{ReO}_x\text{-Au/CeO}_2$ could catalyze the one-pot reduction of 1,4-AHRY to 1,4-BuD. Even though the 55% yield of 1,4-BuD was lower than that over the combination of ReO_x/C and $\text{ReO}_x\text{-Au/CeO}_2$ catalysts, the reuse of the recovered mixture of $\text{ReO}_x/\text{WO}_3\text{-ZrO}_2$ and $\text{ReO}_x\text{-Au/CeO}_2$ catalysts was possible by calcination at 573 K for 3 h. Similar to the mixed catalyst system of $\text{ReO}_x/\text{C} + \text{ReO}_x\text{-Au/CeO}_2$, $\text{ReO}_x\text{-Au/CeO}_2$ catalyzed the deoxydehydration (DODH) reaction of 1,4-AHRY to 2,5-dihydrofuran (2,5-DHF), and $\text{ReO}_x/\text{WO}_3\text{-ZrO}_2$ catalyzed the subsequent reactions of 2,5-DHF to 1,4-BuD. The lower

yield of 1,4-BuD was accompanied by larger formation of THF, which can be due to the disproportionation of 2,5-DHF to THF and furan over the $\text{WO}_3\text{-ZrO}_2$ support, the hydrogenation of 2,5-DHF over $\text{ReO}_x/\text{WO}_3\text{-ZrO}_2$, and cyclization of 1,4-BuD. The performance of $\text{ReO}_x/\text{WO}_3\text{-ZrO}_2$ in the reaction of 2,5-DHF strongly depended on the W loading amount, while the type of crystal structure of ZrO_2 (monoclinic or tetragonal) had little effect. Too much WO_x above the level for monolayer coverage of the ZrO_2 support sharply decreased the activity of Re species in isomerization of 2,5-DHF to 2,3-DHF which is the first step and the most important step in the conversion of 2,5-DHF to 1,4-BuD. The Re species were suggested to be highly dispersed on the WO_3 (sub)monolayer on ZrO_2 , and they can be the active sites for 2,5-DHF disproportionation to 2,3-DHF.

Conflicts of interest

There are no conflicts of interest to declare.

Acknowledgements

This work was supported by JSPS KAKENHI 18H05247. Part of this work was carried out on commission by the Ministry of the Environment, Japan, as "Demonstration project for plastics resource circulation system for decarbonized society".

References

- 1 F. M. Girio, C. Fonseca, F. Carvalheiro, L. C. Duarte, S. Marques and R. Bogel-Lukasik, *Bioresour. Technol.*, 2010, **101**, 4775–4800.
- 2 A. M. Ruppert, K. Weinberg and R. Palkovits, *Angew. Chem., Int. Ed.*, 2012, **51**, 2564–2601.
- 3 M. Besson, P. Gallezot and C. Pinel, *Chem. Rev.*, 2014, **114**, 1827–1870.
- 4 H. Shi, *ChemCatChem*, 2019, **11**, 1824–1877.
- 5 S. Kim, E. E. Kwon, Y. T. Kim, S. Jung, H. K. Kim, G. W. Huber and J. Lee, *Green Chem.*, 2019, **21**, 3715–3743.
- 6 J. J. Bozell and G. R. Petersen, *Green Chem.*, 2010, **12**, 539–554.
- 7 Y. Nakagawa and K. Tomishige, *Catal. Sci. Technol.*, 2011, **1**, 179–190.
- 8 Y. Nakagawa, M. Tamura and K. Tomishige, *J. Mater. Chem. A*, 2014, **2**, 6688–6702.
- 9 D. Sun, Y. Yamada, S. Sato and W. Ueda, *Appl. Catal., B*, 2016, **193**, 75–92.
- 10 Y. Nakagawa, M. Tamura and K. Tomishige, *Res. Chem. Intermed.*, 2018, **44**, 3879–3903.
- 11 Y. Nakagawa, T. Kasumi, J. Ogihara, M. Tamura, T. Arai and K. Tomishige, *ACS Omega*, 2020, **5**, 2520–2530.
- 12 Y. Amada, H. Watanabe, Y. Hirai, Y. Kajikawa, Y. Nakagawa and K. Tomishige, *ChemSusChem*, 2012, **5**, 1991–1999.
- 13 A. Said, D. D. S. Perez, N. Perret, C. Pinel and M. Besson, *ChemCatChem*, 2017, **9**, 2768–2783.
- 14 T. Arai, M. Tamura, Y. Nakagawa and K. Tomishige, *ChemSusChem*, 2016, **9**, 1680–1688.
- 15 Z. Huang, K. J. Barnett, J. P. Chada, Z. J. Brentzel, Z. Xu, J. A. Dumesic and G. W. Huber, *ACS Catal.*, 2017, **7**, 8429–8440.
- 16 J. B. McKinlay, C. Vieille and J. G. Zeikus, *Appl. Microbiol. Biotechnol.*, 2007, **76**, 727–740.
- 17 D. R. Vardon, A. E. Settle, V. Vorotnikov, M. J. Menart, T. R. Eaton, K. A. Unocic, K. X. Steirer, K. N. Wood, N. S. Cleveland, K. E. Moyer, W. E. Michener and G. T. Beckham, *ACS Catal.*, 2017, **7**, 6207–6219.
- 18 D. Sun, S. Sato, W. Ueda, A. Primo, H. Garcias and A. Corma, *Green Chem.*, 2016, **18**, 2579–2597.
- 19 M. Tamura, Y. Nakagawa and K. Tomishige, *Asian J. Org. Chem.*, 2020, **9**, 126–143.
- 20 Y. Nakagawa, Y. Shinmi, S. Koso and K. Tomishige, *J. Catal.*, 2010, **272**, 191–194.
- 21 L. Liu, S. Kawakami, Y. Nakagawa, M. Tamura and K. Tomishige, *Appl. Catal., B*, 2019, **256**, 117775.
- 22 L. Liu, T. Asano, Y. Nakagawa, M. Tamura, K. Okumura and K. Tomishige, *ACS Catal.*, 2019, **9**, 10913–10930.
- 23 T. Wang, S. Liu, M. Tamura, Y. Nakagawa, N. Hiyoshi and K. Tomishige, *Green Chem.*, 2018, **20**, 2547–2557.
- 24 J. R. Dethlefsen and P. Fristrup, *ChemSusChem*, 2015, **8**, 767–775.
- 25 A. R. Petersen and P. Fristrup, *Chem. – Eur. J.*, 2017, **23**, 10235–10243.
- 26 S. Raju, M. Moret and R. J. M. K. Gebbink, *ACS Catal.*, 2015, **5**, 281–300.
- 27 L. Sandbrink, E. Klindtworth, H.-U. Islam, A. M. Beale and R. Palkovits, *ACS Catal.*, 2016, **6**, 677–680.
- 28 L. Sandbrink, K. Beckerle, I. Meiners, R. Liffmann, K. Rahimi, J. Okuda and R. Palkovits, *ChemSusChem*, 2017, **10**, 1375–1379.
- 29 Y. Kon, M. Araque, T. Nakashima, S. Paul, F. Dumeignil and B. Katryniok, *ChemistrySelect*, 2017, **2**, 9864–9868.
- 30 B. E. Sharkey and F. C. Jentoft, *ACS Catal.*, 2019, **9**, 11317–11328.
- 31 J. Lin, H. Song, X. Shen, B. Wang, S. Xie, W. Deng, D. Wu, Q. Zhang and Y. Wang, *Chem. Commun.*, 2019, **55**, 11017–11020.
- 32 S. Tazawa, N. Ota, M. Tamura, Y. Nakagawa, K. Okumura and K. Tomishige, *ACS Catal.*, 2016, **6**, 6393–6397.
- 33 Y. Nakagawa, S. Tazawa, T. Wang, M. Tamura, N. Hiyoshi, K. Okumura and K. Tomishige, *ACS Catal.*, 2018, **8**, 584–595.
- 34 J. Cao, M. Tamura, Y. Nakagawa and K. Tomishige, *ACS Catal.*, 2019, **9**, 3725–3729.
- 35 K. Tomishige, Y. Nakagawa and M. Tamura, *Chin. Chem. Lett.*, 2020, **31**, 1071–1077.
- 36 N. Ota, M. Tamura, Y. Nakagawa, K. Okumura and K. Tomishige, *Angew. Chem., Int. Ed.*, 2015, **54**, 1897–1900.
- 37 N. Ota, M. Tamura, Y. Nakagawa and K. Tomishige, *ACS Catal.*, 2016, **6**, 3213–3226.
- 38 M. Tamura, N. Yuasa, J. Cao, Y. Nakagawa and K. Tomishige, *Angew. Chem., Int. Ed.*, 2018, **57**, 8058–8062.
- 39 T. Wang, M. Tamura, Y. Nakagawa and K. Tomishige, *ChemSusChem*, 2019, **12**, 3615–3626.
- 40 B. Zhang, Z. Qi, X. Li, J. Ji, W. Luo, C. Li, A. Wang and T. Zhang, *ACS Sustainable Chem. Eng.*, 2019, **7**, 208–215.
- 41 B. Zhang, Z. Qi, X. Li, J. Ji, L. Zhang, H. Wang, X. Liu and C. Li, *Green Chem.*, 2019, **21**, 5556–5564.

- 42 R. Pinkos, R. H. Fischer, B. Breitscheidel and P. Polanek, *CA Pat.*, 2168458C, 2004.
- 43 S. Ramu, N. Lingaiah, B. L. A. P. Devi, R. B. N. Prasad, I. Suryanarayana and P. S. S. Prasad, *Appl. Catal., A*, 2004, **276**, 163–168.
- 44 M. Rønning, T. Gjervan, R. Prestivik, D. G. Nicholson and A. Holmen, *J. Catal.*, 2001, **204**, 292–304.
- 45 Y. Takeda, M. Tamura, Y. Nakagawa, K. Okumura and K. Tomishige, *ACS Catal.*, 2015, **5**, 7034–7047.
- 46 E. I. Ross-Medgaarden, W. V. Knowles, T. Kim, M. S. Wong, W. Zhou, C. J. Kiely and I. E. Wachs, *J. Catal.*, 2008, **256**, 108–125.
- 47 T. Yamamoto, A. Teramachi, A. Orita, A. Kurimoto, T. Motoi and T. Tanaka, *J. Phys. Chem. C*, 2016, **120**, 19705–19713.